

# We are IntechOpen, the world's leading publisher of Open Access books Built by scientists, for scientists

4,800

Open access books available

122,000

International authors and editors

135M

Downloads

Our authors are among the

154

Countries delivered to

TOP 1%

most cited scientists

12.2%

Contributors from top 500 universities



WEB OF SCIENCE™

Selection of our books indexed in the Book Citation Index  
in Web of Science™ Core Collection (BKCI)

Interested in publishing with us?  
Contact [book.department@intechopen.com](mailto:book.department@intechopen.com)

Numbers displayed above are based on latest data collected.  
For more information visit [www.intechopen.com](http://www.intechopen.com)



# Reinforcement of Austenitic Manganese Steel with (TiMo) Carbide Particles Previously Synthesized by SHS

Jose Ignacio Erasquin  
Tecnalia Research and Innovation  
Spain

## 1. Introduction

Production parameters and the properties or final characteristics of each particular material are interrelated, as well as the service performance of the manufactured product. Then, a possible scheme to continue in the process of optimization/design of materials is shown in Figure 1. The two basic steps for this would be the following: a) Cause-Effect Relationship: Analysis and study of the effects of the manufacturing process of the material (composition, refining, solidification, heat treatment, etc.) in the micro or nano-structure (phases, constituents, grain size, etc.), of this structure in the mechanical properties (toughness, hardness), and of these in the final performance of the product in service (fatigue, impact, creep failures, wear, deformation, corrosion, etc...); b) Objective-Means Relationship: In reverse order to the previous definition, to optimize the mechanical properties for the desired behavior in service identifying the micro-nano structural parameters that govern such characteristics (particles of second phase, martensite on laths, etc.), in order to establish the best production process to obtain the desired material in each case once designed and defined its optimal internal parameters.

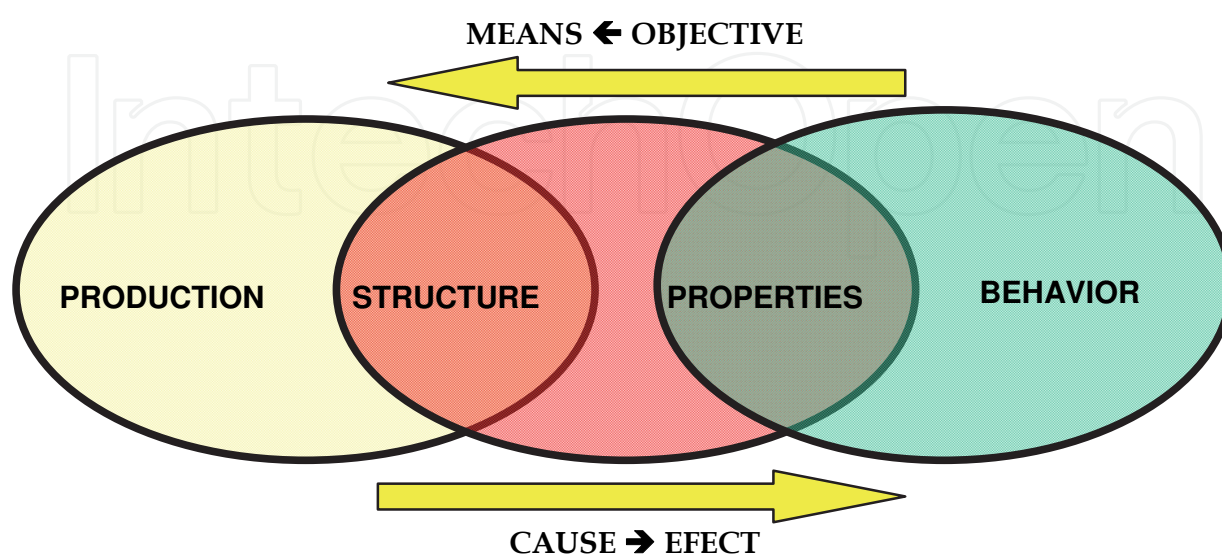


Fig. 1. Scheme for optimization/design of materials

In this context, the main priorities for improving the mechanical properties of materials, in general, can be simplified into two main groups: Those aiming to increase its mechanical strength, stiffness and toughness; Those that can lead to an increase in fracture toughness of the material. Latter consists in adding second phase particles embedded in the matrix, which generate energy absorbing processes during the growth of cracks in the matrix as well as acting as a barrier to it and the movement of dislocations, while the mechanical strength is increased, among other factors, with decreasing grain size of the microstructure. The elastic constants, on the other hand, increases with a higher ratio "length / diameter" of the second phase particles (Tinklepaugh & Crandall, 1960). The development of these materials leads to the so-called composed materials or "composites." With this term is called, in general, a material made by a constituent discrete (reinforcement) distributed and dispersed in a continuous phase (matrix) and whose characteristics are a function of both constituents, the geometry and structure of them and the properties of its boundaries or interfaces (Steen, 1992). Among the wide variety of these composite materials (classified, on the one hand, based on physical or chemical nature of the matrix and, secondly, in terms of continuous or discontinuous reinforcement), one of the major groups is the conformed by those whose higher fraction is a metal, owing to the superiority of some of its properties compared with those of ceramic matrix material (toughness and ductility) and organic matrix (high temperature resistance, hardness, etc.). In the former ones, the constituent of reinforcement is usually non-metallic, predominantly ceramic. About the geometry of the reinforcement, some of the metal matrix composites most commonly used are those known (Chesney, 1990) as: a) Metals reinforced with continuous fibers, parallel or not, and a diameter of less than 20 microns; b) Metals reinforced with short fibers, staple, and "whiskers"; c) Metals reinforced with particles, approximately equiaxed. All types are presented in Figure 2.

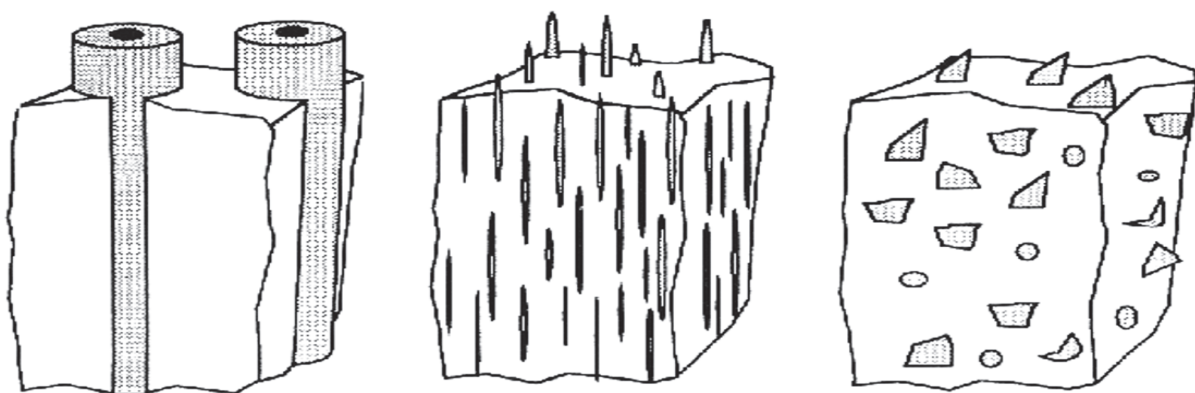


Fig. 2. Metallic matrix reinforcement types.

In this sense, in the last 30 years almost all efforts have focused on composites of low melting point alloys (Al, Ti, Mg, Cu), being the most developed ones the aluminum alloys containing particles of SiC or alumina and the titanium alloys with carbides and borides (Kelly & Macmillan, 1987; Terry & Chinyamakobvu, 1992). At the end of 80<sup>th</sup> start the first attempts in order to produce ferrous materials reinforced with constituents more hard, added after its previous synthesis. R.M. Hathaway et al., in your "Ferrous Composites: a Review" (Hathaway et al., 1997), revise the development achieved in this matter (until 1997) by powder metallurgy process as well as liquid metallurgy one. Subsequently, Tecnalia

Research and Innovation (Agote et al., 2005; Erausquin et al., 2009; Erausquin, 2009) have studied the possibility of developing such other iron matrix (steels), in order to combine in one material at the macroscopic level, the ductility, toughness, etc., related to them, with the hardness (translated into greater wear resistance) and stiffness (translated into greater yield strength and creep) of the strengthening particles. However, apart from a few later publications in this line of steel with carbide and borides particles previously developed (Nutting, 1998; Bates et al., 1998; Galgali et al., 1999; Degnan & Shiway, 2002) and others relating to training "in-situ" the precipitation, from alloying elements, of TiC particles in ferrous materials (Das et al., 2005; Dogan et al., 2006), there is hardly any progress on the matter. One proper steel alloy to be intended to reinforce is the Hadfield type steel because the austenite of this manganese steel (1.0-1.4%C; 12-14%Mn), even though able to be hardened by impact, explosion, etc., is very ductile, tough and deformable, so that the industrial parts made with this material often suffer important geometric deformations during its work. To minimize this problem, it is necessary to insert harder particles in the matrix in order to increase the austenite stiffness preserving it sufficient toughness. Refractory metal carbides as Titanium, Tungsten or Zirconium carbides are the most common ceramic elements used for these applications (Steen, 1992), because the carbides of the transition metals in Groups IV - VI have extremely high melting points and are therefore referred to collectively as the "refractory carbides." In addition to their stability at high temperatures, these compounds are extremely hard, finding industrial use in cutting tools and wear-resistant parts. Their hardness is retained to very high temperatures, and they have low chemical reactivity (they are attacked only by concentrated acid or base in the presence of oxidizing agents at room temperature), and retain good corrosion resistance to high temperatures. The refractory carbides are strong, with Young's modulus values (a measure of elastic deformation resistance) rivalling those of SiC at room temperature. In addition, they have good thermal shock resistance and good thermal conductivity, permitting heat to be drawn away from the working surface of the tool. This gives them a benefit over other refractory materials, which do not conduct heat so well (Storms, 1967; Toth, 1971). Most of the transition metal monocarbides form in the *B1* (NaCl) structure, *fcc* metal with carbon occupying the octahedral interstitial sites. The shortest M-M distance is about 30% greater in the *B1* carbide than in the pure metal for the Group IV and V carbides, but drops to less than 10% greater for the Group VI or VII carbides. At 100% site occupancy, the stoichiometry of the carbide is  $MC_{1.0}$ , though this situation is rarely realized. The concentration and ordering, if any, of the vacancies that result from a nonstoichiometric M-C ratio have a great effect on the thermodynamic, mechanical, electronic, and magnetic properties of the metal carbides; however, the details of these effects are a matter of some debate in the literature, due to the difficulties inherent in synthesizing pure compounds and in measuring the exact details of the crystal structure of a given sample (Storms, 1967). In this field, one of the most attractive reinforcing ceramic constituent is the titanium carbide, because of its high hardness, thermal stability and low density. But the low wettability and segregation tendency (Terry & Chinyamakobvu, 1992; Wood et al., 1995) of these carbide particles make them technically difficult to incorporate into manufactured or semi manufactured metallic alloys, cermets or coating materials.

Indeed, the development of a liquid metallurgy process enabling the reinforcement by means of the addition of the ceramic material to the molten metal in the melting furnace would become an important advance in this field. Nevertheless, these titanium carbide products are also prone to the coalescence and have poor wettability into molten bath, so

that, the resulting operation yield and the subsequent property improvement is very low. These disadvantages are solved if the ceramic particle is a complex carbide  $(\text{TiMo})\text{C}$ , if it is bonded by metallic Fe, having a masteralloy of  $\text{Fe}(\text{TiMo})\text{C}$  type, and making this masteralloy by self-propagated high temperature synthesis (SHS). After that, its addition to the liquid austenitic manganese steel, the pouring of the mix (steel+carbides), its solidification, for example in sand molds, and the subsequent heat treatment (solution annealing and rapid quenching) produces composite castings or parts composed by a matrix of austenite and discrete carbide particles of  $(\text{TiMo})\text{C}$  inserted in it (Erasquin et al., 2009). This chapter describes the necessary process for it and the characteristics of the obtained products.

## 2. Experimental

The process includes the following fundamental steps: 1) Previous preparation of the material of reinforcement, in this case a masteralloy of  $\text{Fe}(\text{MoTi})\text{C}$  type. 2) Melting of the high carbon high manganese steel bath by means of conventional electric furnace and addition of the masteralloy to the molten steel bath. 3) Pouring, solidification and heat treatment of the “composite” product.

### 2.1 Masteralloy synthesis

The masteralloy is synthesized by self-propagating high temperature synthesis using raw materials containing Fe, Ti, Mo and C. This process allows obtaining products with very low energetic consumption and high purity, favourable this parameter for the wettability. The SHS, or materials synthesis by combustion, is based in exothermic chemical reactions solid+solid or solid+gas and the heat generated in the reaction allows its self-propagation by means a wave or combustion front (Tamburini et al., 2000). The full process is indicated in the figure 3.

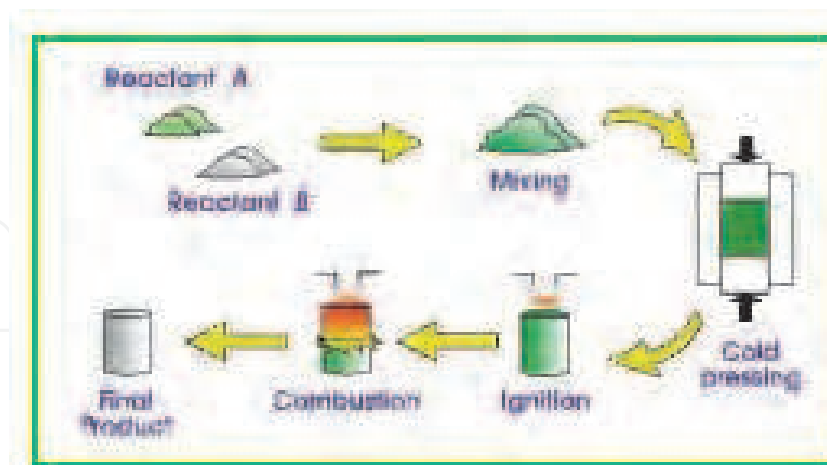


Fig. 3. Full process for SHS (Tamburini et al., 2000)

The figure 4 shows the selfpropagating synthesis of the  $\text{NiAl}$  intermetallic in air atmosphere.

The exothermic power of a reaction is deduced from the Ellingham diagrams, as the figure 5 for the carbides formation. At less  $\Delta G$ , more exothermic is the reaction, as the case of the synthesis of  $\text{TiC}$



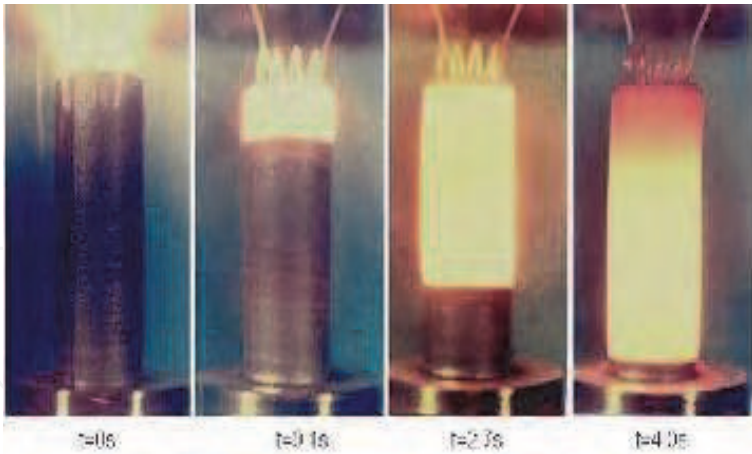


Fig. 4. NiAl SHS (Courtesy of ISMAN Institute of Moscow)

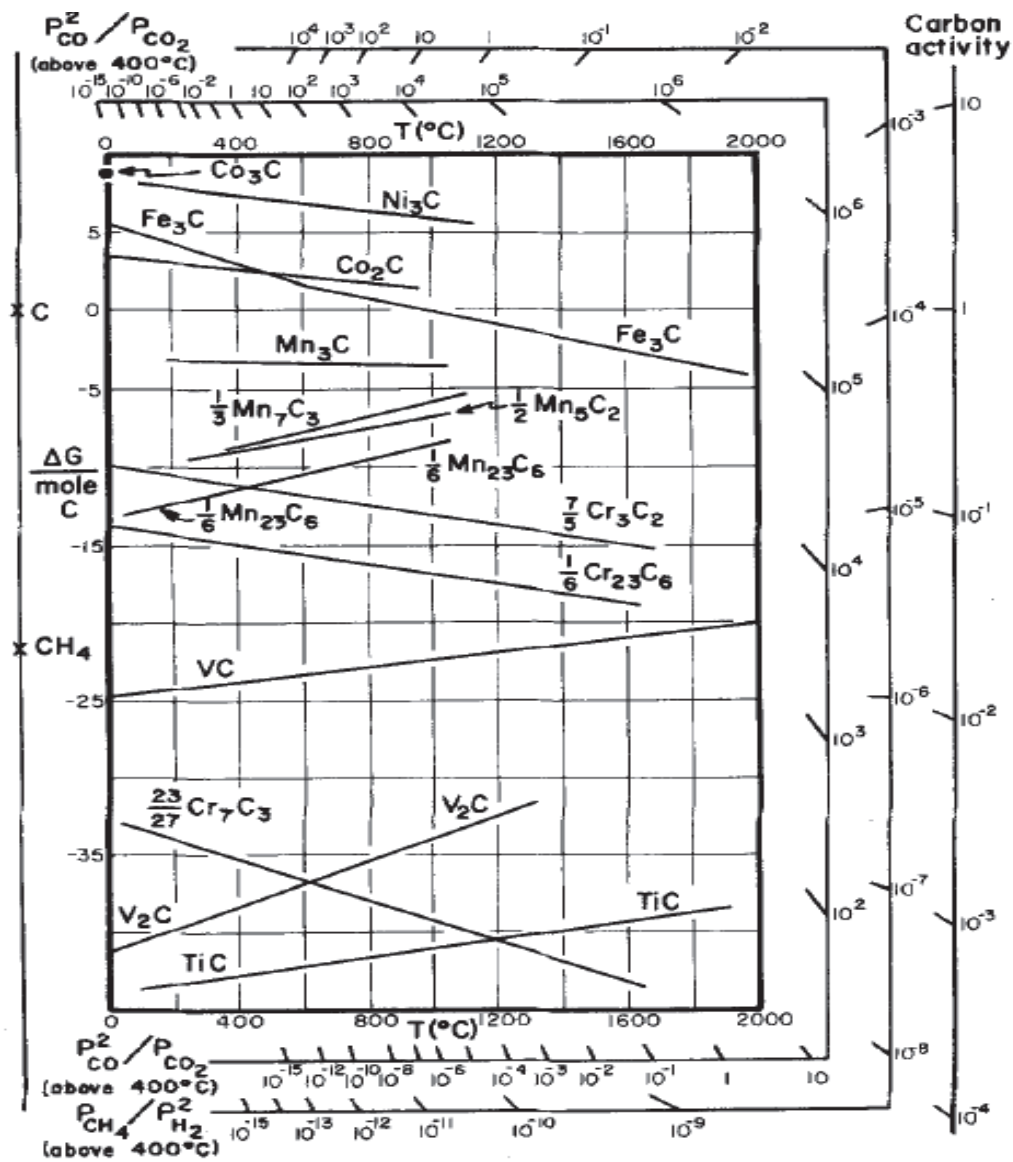


Fig. 5. Ellingham diagram of carbides formation (Shatynski, 1979)

Also, although AG values for the formation of the molybdenum carbides are positives at room temperature, at high temperature these values are very negatives (low AG) as we can see in the figure 6. This fact facilitates the insertion de molybdenum atoms within titanium carbide cell (Erausquin, 2009).

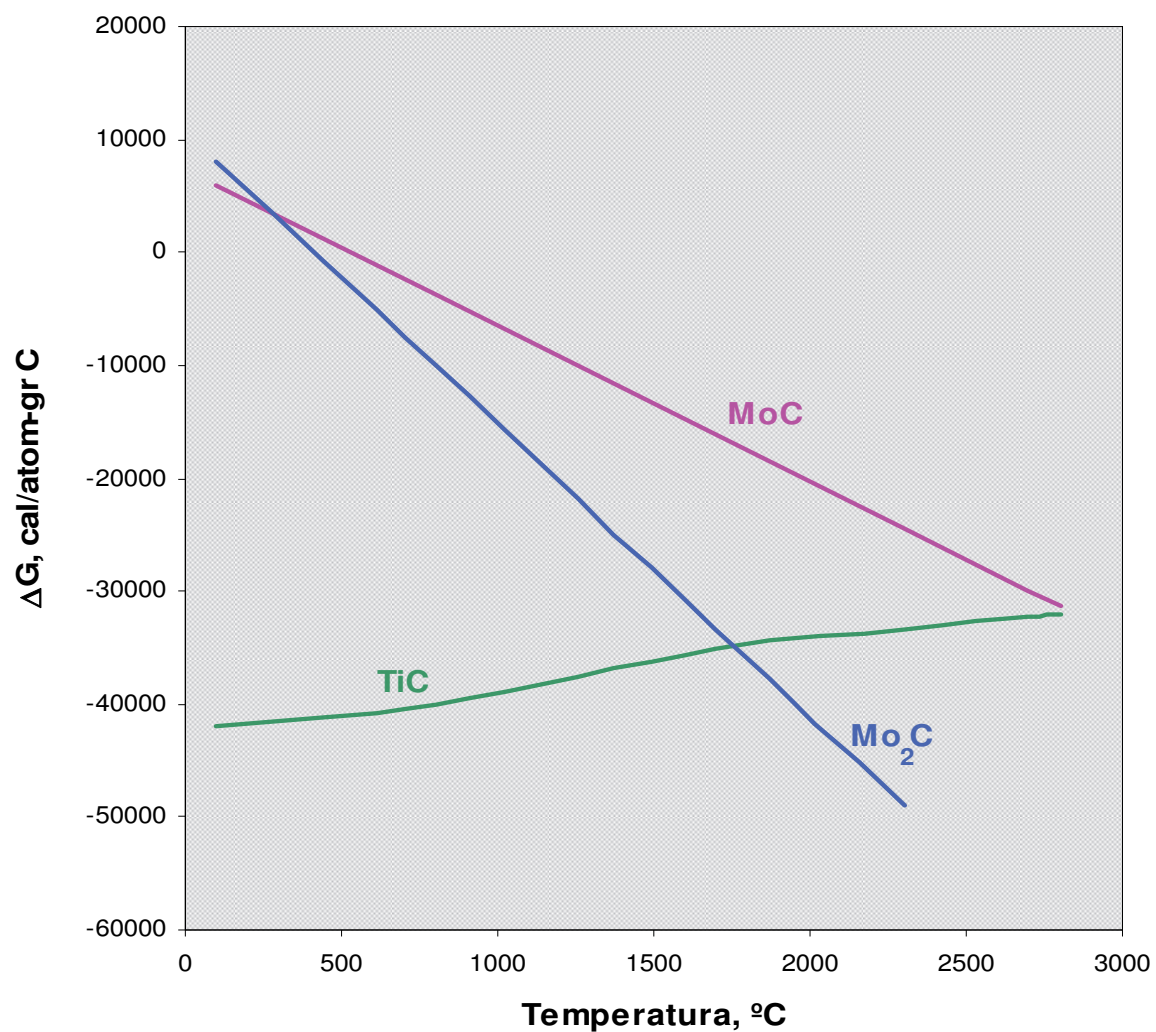


Fig. 6. Ellingham diagram of titanium and molybdenum carbides formation (Erausquin, 2009)

In the present work, the raw materials, its quantities and its characteristics are the next: 12% pure Carbon of 1-3  $\mu$  of grain size; 73% FeTi (67-70% Ti; 5% Al; remainder: Fe), crushed to 100  $\mu$  of grain size; and 15% FeMo (66% Mo; 1% Si; remainder: Fe), crushed to 100  $\mu$  of grain size. Mixed the three materials and pressed the mix to 4-6MPa., the synthesis is made in a steel reactor with argon atmosphere and a wolfram resistance in an edge. The heat of this resistance produces the start of the reaction and after that this one is propagated in wave front due the formation heat of the masteralloy, taking place the total mix synthesis (Erausquin et al., 2009). At macroscopic level, the resultant masteralloy is a brittle and porous material, with ceramic aspect (Erausquin et al., 2009).

The figures 7, 8 and 9 show the SHS equipment, the product formation, and the synthesis propagation, respectively.



Fig. 7. Powder mixer (left); Powder press (centre); SHS reactor (right)

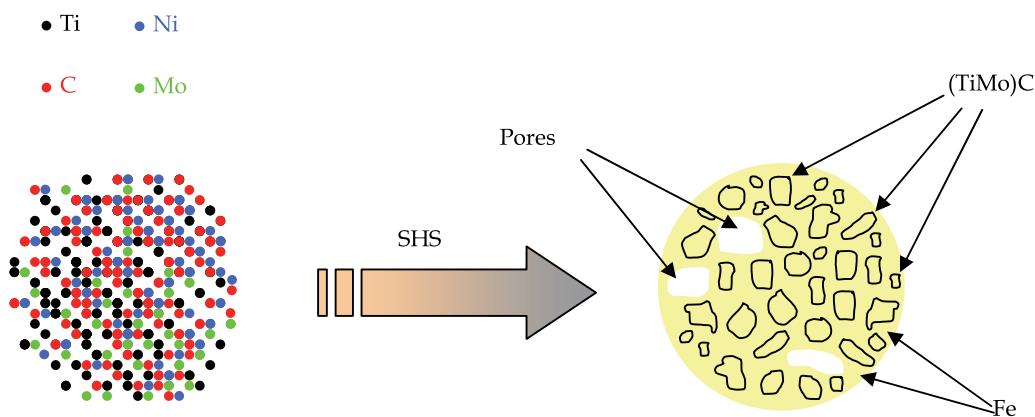


Fig. 8. Masteralloy formation (Erausquin, 2009)

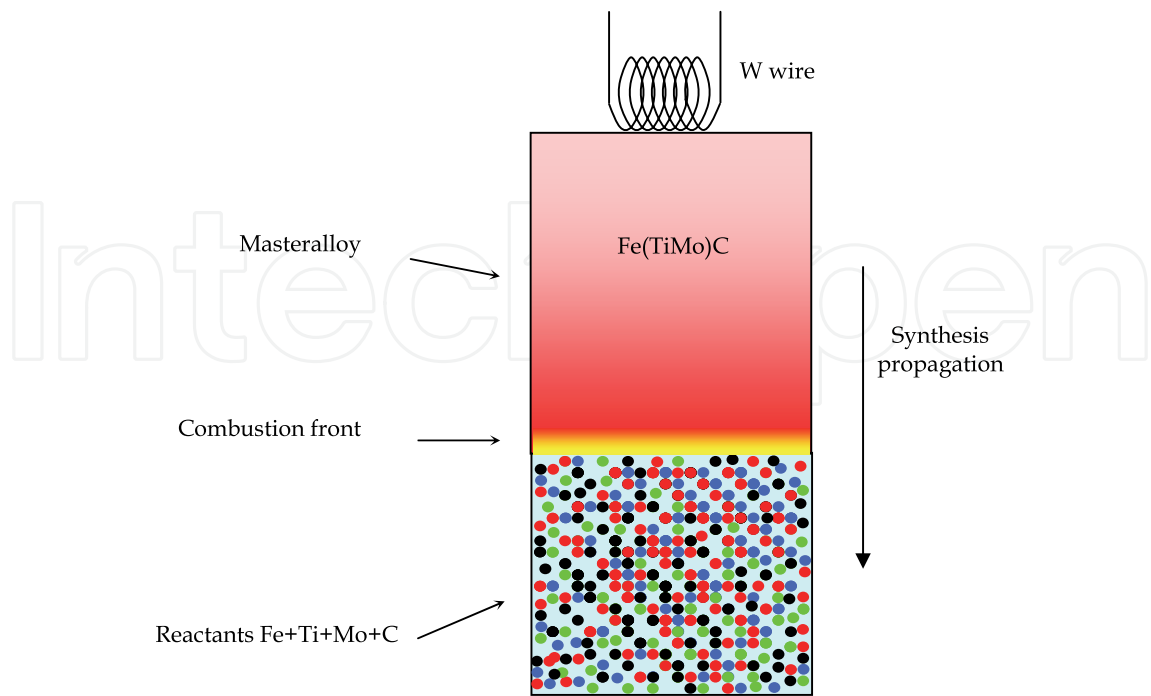


Fig. 9. Synthesis self-propagation



2.2 Melting of steel and masteralloy addition

The base austenitic steel is obtained by melting, in an induction furnace of 300 Kg. of capacity and 1000 Hz. of frequency, the next raw materials and quantities: 83% carbon steel scrap; 13% Fe-Mn high carbon and 4% Fe-Mn low carbon, in order to achieve the chemical composition, in % mass, of the table 1.

C	Si	Mn	P	S	Cr	Ni	Mo
1.00-1.20	0.30	12.0-14.0	0.035	0.010	-	-	-

Table 1. Chemical composition (% mass) of the base steel

The process include the next steps (Erausquin et al., 2009): Melting of the raw materials in the furnace and heating of the liquid alloy up to 1873°K.; Addition of the reinforcing material, consisting in a 10% of weight, over the base steel, of masteralloy Fe(TiMo)C previously crushed to 2-20 mm. grain size; After that, heating the bath (steel+carbides) up to pouring temperature (about 1823°K).

2.3 Pouring, solidification and heat treatment

The resulting liquid material, steel alloy + reinforcing carbides, can be poured to produce ingots o castings. In this case, we have obtained sample-blocks and industrial castings solidified in sand molds. After that, these ones have been heat treated (solution annealing at 1373°K and rapid quenching in water), as the same manner that a conventional austenitic manganese steel product. The samples for metallographic and mechanical tests have been prepared from this heat treated material.

The reinforcement full process is schematized in the figure 10.

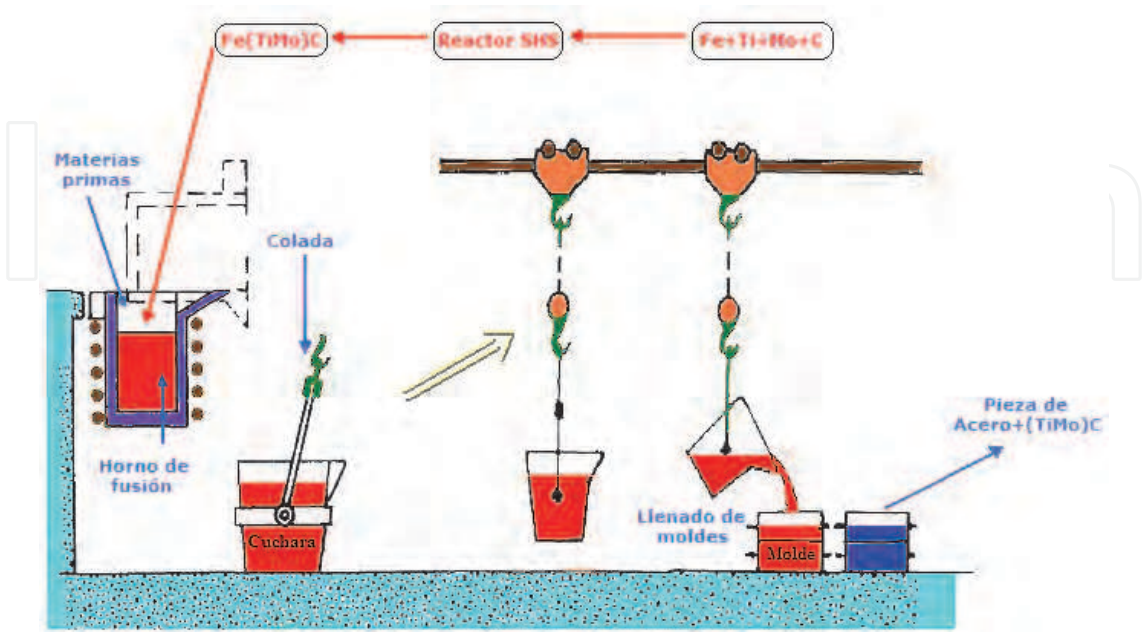


Fig. 10. Reinforcement process

The figures 11 and 12 show the alloy preparation and pouring, and the mould filling steps, respectively.

The figure 13 shows the mould filled with reinforced steel.



Fig. 11. Masteralloy addition and pouring of steel+carbides



Fig. 12. Mould filling with steel+carbides





Fig. 13. Mould filled with steel+carbides

## 2.4 Characterization

The metallographic characterization has been made by means of optic and electronic microscopy (SEM with analytical equipment EDS), while the mechanical properties have been tested by means of a Vickers microhardness tester FM-100, tensile test machine Instron 8034, Charpy test machine Tinius Olsen model 74 and a pin on disk tribometre Biceri (05-168.02) for wear test. Also, we have used the diffractometer Siemens D-500 in order to obtain the X ray diffraction diagram of samples of masteralloy finely crushed. The peaks of crystallographic planes of the resultant diffraction tests are contrasted and compared with those of the JCPDS (Joint Committee Pattern for Diffraction Standards).

## 3. Results

### 3.1 Masteralloy

The visual aspect of the masteralloy produced by SHS is shown in figure 14.



Fig. 14. Blocks of masteralloy Fe(TiMo)C

In the figure 15 is presented the masteralloy crushed (left), and polished (right). In this one, we can see two constituents: the binder (white) and the polygonal-rounded particles (grey).

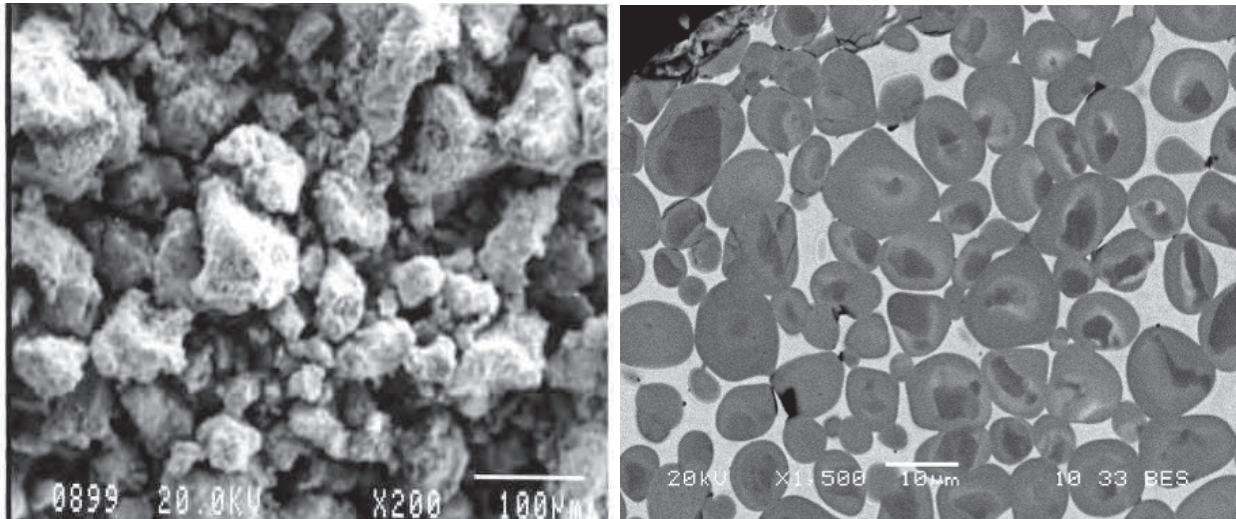


Fig. 15. Masteralloy crushed (left), and polished (right)

The figure 16 shows the spectra of the white constituent or binder (left), and of the grey particle (right). From them, we can deduce that the binder is iron, while the particles could be complex carbides of titanium and molybdenum. The semiquantitative chemical composition (obtained by EDS) of these particles is presented in the table 2.

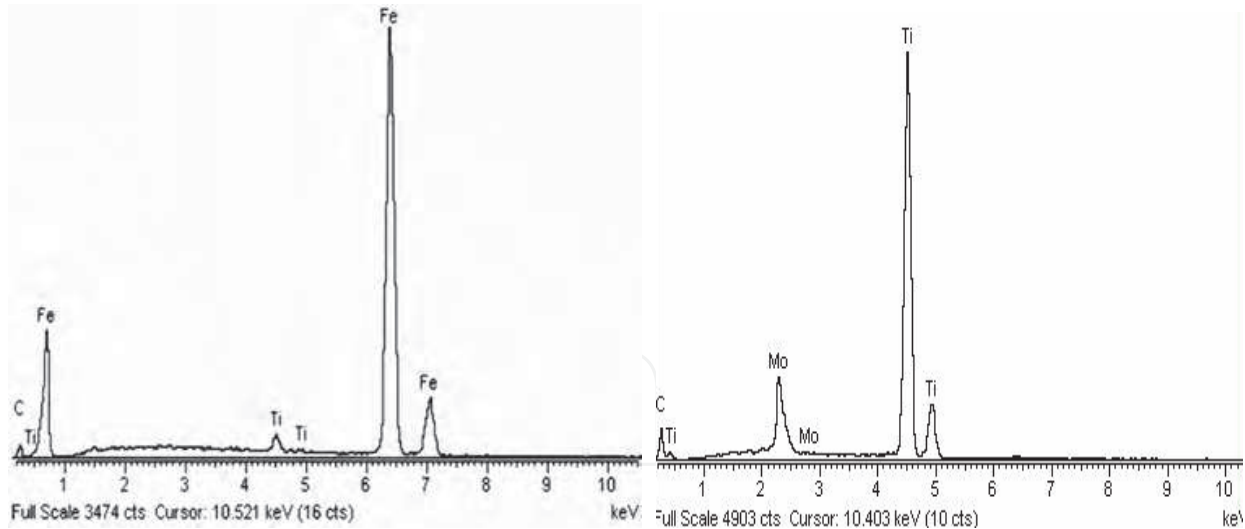


Fig. 16. Binder spectrum (left), particle spectrum (right)

Spectrum Label	C	Al	Ti	Fe	Mo	Total
Grey particle	18.43		68.07		13.50	100.00

Table 2. Semicuantitative composition (% mass) of the masteralloy grey particles

Besides these results, by means of the X ray diffraction tests we can demonstrate (Erausquin, 2009) the grey particles of the masteralloy are carbides of (TiMo)C type, because being unknown the  $\theta$  angle of this complex carbide, the peak of diffraction results in the TiC angle, as is indicated in the figure 17.

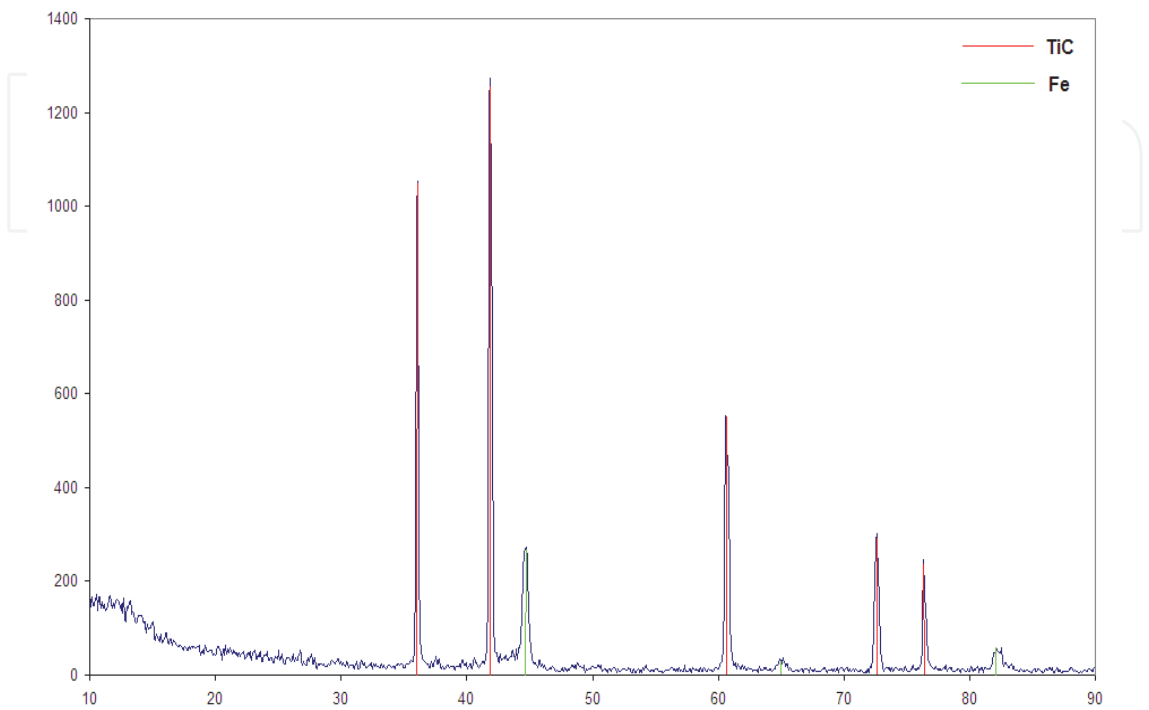


Fig. 17. X ray diffraction of the masteralloy

So that, if the reactants of a SHS reaction are C and Ti, the product is the monocarbide TiC, while if we add a small quantity of Mo to the mix, the result of the synthesis is the complex (TiMo)C, with the same crystallographic configuration as the former, but substituting a few atoms of Ti (green) by Mo ones (red), as indicated in the figures 18 and 19 (Erausquin, 2009).

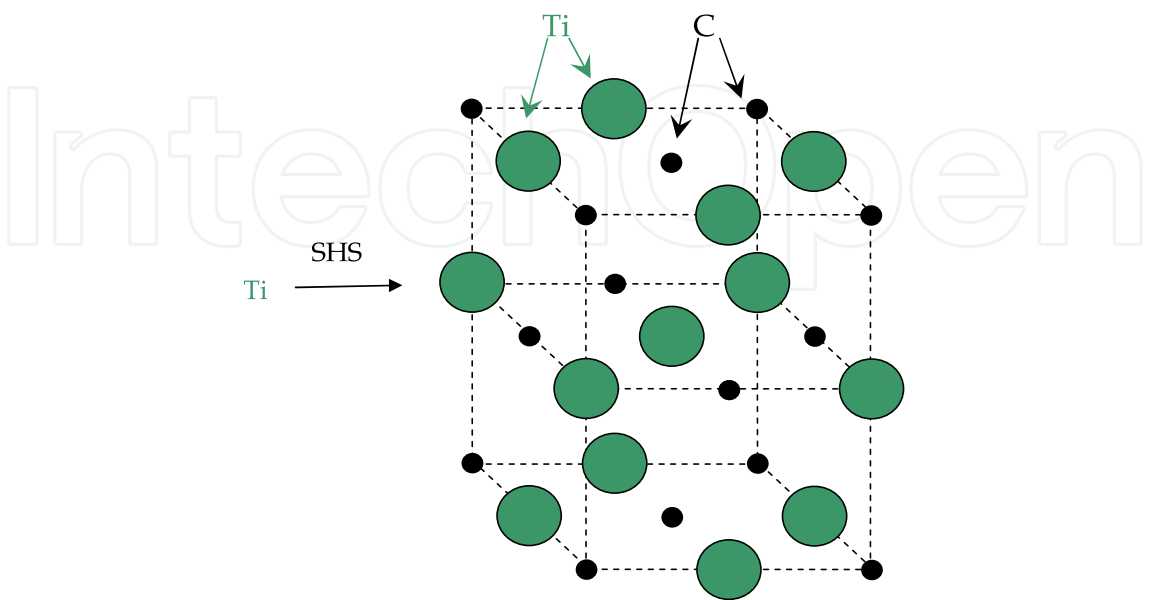


Fig. 18. TiC synthesis



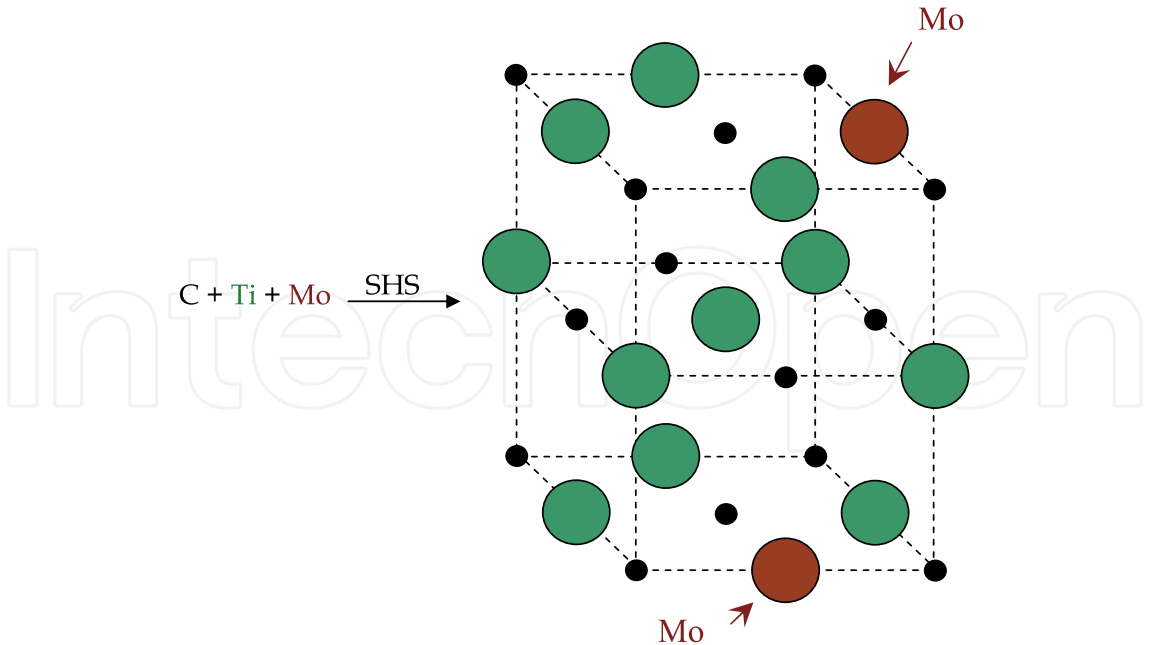


Fig. 19. (TiMoC synthesis

**3.2 Reinforced steel**

The mechanism of reinforcement of the steel by the carbides of the masteralloy is schematized in the figure 20.

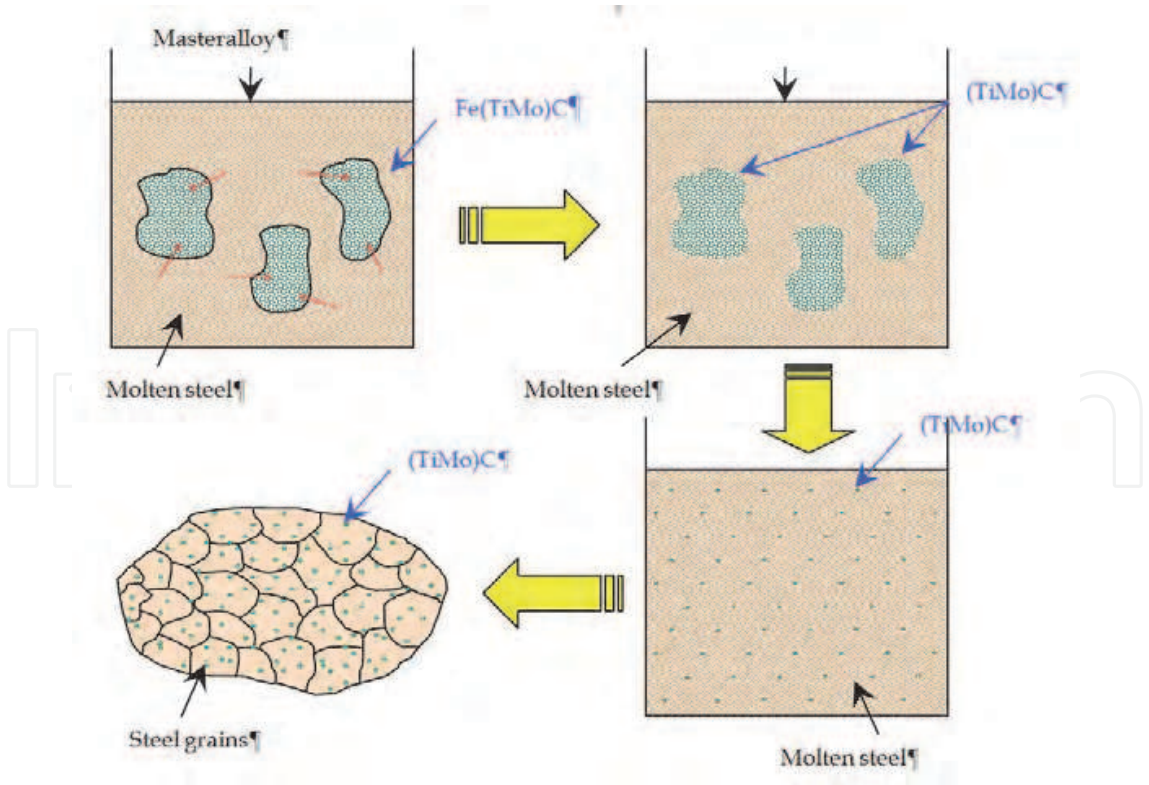


Fig. 20. Carbide reinforcement of the steel

In the figure 21 are shown the castings (hammers for crushing stone) of reinforced steel and in the figure 22, three hammers working in a rotary mill.



Fig. 21. Castings of reinforced steel



Fig. 22. Three experimental hammers in a rotary mill



**3.2.1 Microstructure of the reinforced steel**

The figure 23 shows the microstructure (unetched) of the reinforced austenitic steel (left), and the same but obtained with images analyser (right, x400)). In both, we can see discrete, microscopic and polygonal particles (dark grey at left, blue at right) into matrix (light at left, red at right).

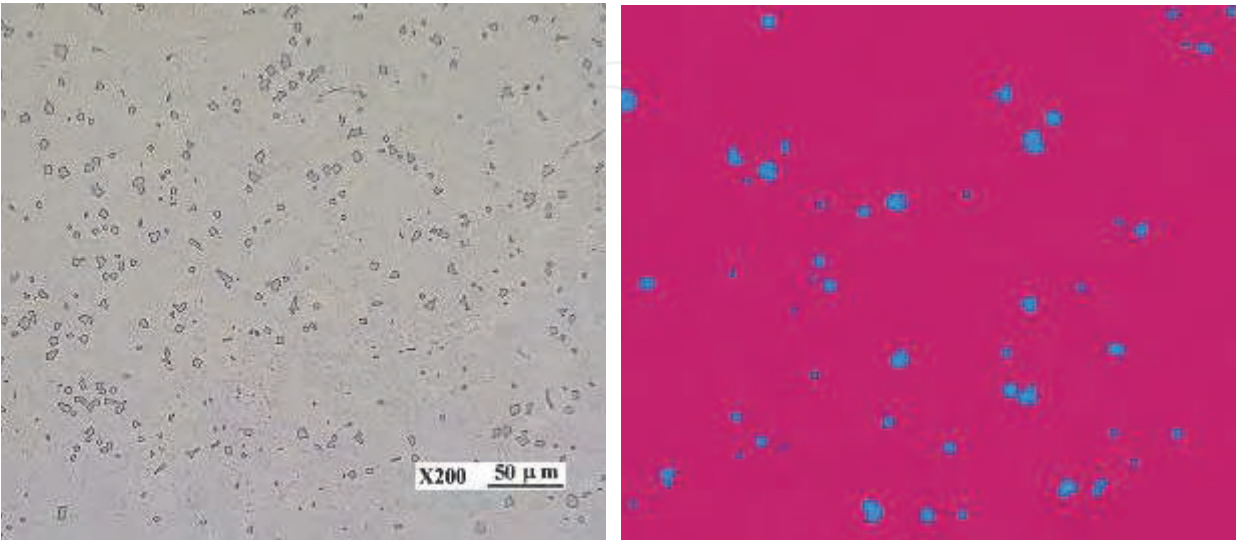


Fig. 23. Microstructure of the reinforced steel

The figure 24 shows the last microstructure, etched, at 40 and 400 magnifications respectively, where we can see the former particles inserted within austenite grains. In the figure 25 we can see the spectra of the matrix of the reinforced steel (left) and of the particles inserted in it (right). Finally, in the tables 3 and 4 are shown the both semiquantitative composition (similar to base steel of the table 1 and to the grey particles of the masteralloy of the table 2, respectively).

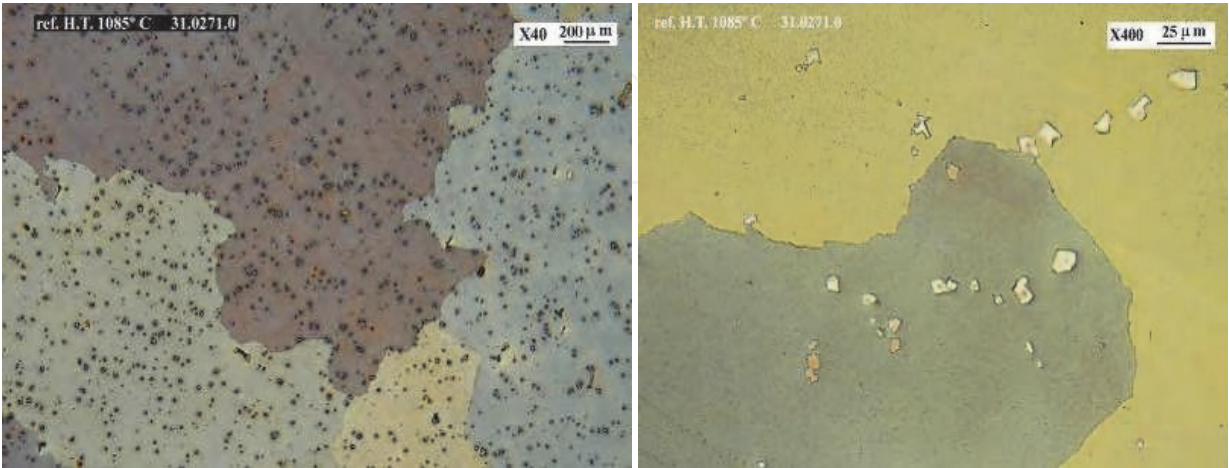


Fig. 24. Microstructure of the reinforced steel

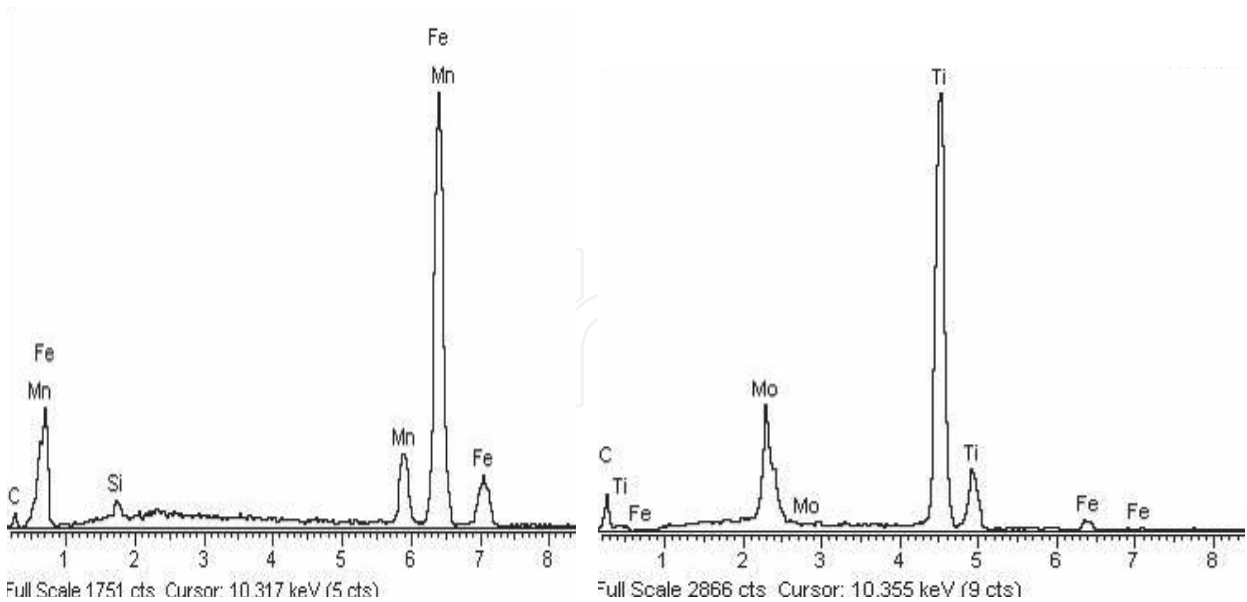


Fig. 25. Matrix spectrum (left) and particle spectrum (right) in the reinforced steel

Spectrum Label	C	Al	Si	Mn	Fe	Total
Steel matrix	1.15		1.14	12.75	84.96	100.00

Table 3. Semicuantitative composition (% mass) of the matrix of the reinforced steel

Spectrum Label	C	Al	Ti	Fe	Mo	Total
Grey particle	18.62		61.00	2.57	17.81	100.00

Table 4. Semicuantitative composition (% mass) of the particles of the reinforced steel

From them, we can deduce that these particles could be titanium and molybdenum complex carbides. Their chemical composition (semicuantitative, obtained by EDS) and that of the grey particles of the masteralloy (table 2) are similar, with a bit more Mo in the former in detriment of the Ti.

3.2.2 Mechanical properties

3.2.2.1 Hardness.

The microhardness values of the polygonal particles inserted in the austenitic grains of the reinforced steel are between 2400 and 3100 HV<sub>0.025</sub>. This indicate the particles are carbides.

3.2.2.2 Tensile and Charpy tests.

In the table 5 we can see the values obtained in these tests (according to the norm EN-ISO 6506-1) for Hadfield conventional steel and the reinforced steel of this work. Of these values we can deduce the reinforced steel is less tough and ductile than the conventional one, although its toughness is certainly enough for a satisfactory behaviour under impact conditions. On the other hand, the yield strength of the reinforced steel is higher and, with

it, we expect the stiffness and the fatigue resistance, two characteristic-lacks of the Hadfield steel, will be increased.

	Tensile strength (MPa)	Yield strength(0.2%) (MPa)	Elongation (%)	Reduction of area (%)	Impact energy (J)
Conventional steel	636	371	35	41	162
Reinforced steel	575	482	16	22	128

Table 5. Mechanical properties of the reinforced steel

3.2.3 Wear resistance

It has been evaluated by means of the pin (of martensitic steel) on disk test on the conventional and reinforced steel samples, during 30 hours under a normal stress of 90 MPa (N/mm2) and 150 rpm. The results, in wear rate of the disks, are in the table 6. From them, we can deduce the wear resistance (under stress) of the reinforced austenitic steel is twice the conventional.

	Hadfield steel	Reinforced steel
Wear rate (mm³ /N m)	6.8 ·10 <sup>-8</sup>	3.5 ·10 <sup>-8</sup>

Table 6. Wear behaviour

4. Conclusions

From the figures 15, 16 and table 2, we can deduce the grey particles of the masteralloy synthesized by SHS are complex carbides of (TiMo)C type. The reaction synthesis is the sum of the next sequential (almost infinitesimal in time) partial reactions:  
Formation of a 68%Ti-32%Fe intermetallic eutectic and it melting at 1086 ° C aprox. due to heat generated by an electrical resistance; Diffusion of solid C in the Ti-Fe liquid and formation of TiC (very exothermic reaction with spontaneous generation of heat, rising the temperature, while Fe remains as binder phase);Replacement, in the TiC cell, of some Ti atoms by Mo ones, because the atomic radii values are similar (1,40-1,47 Å of the Ti, 1,39-1,45 Å of the Mo) and at high temperature the combination of C and Mo is very favourable. Then, TiC+Mo+Fe → Fe(TiMo)C.  
From the microstructure (fig. 23 and 24), the spectra (fig. 25, table 4) and the microhardness values (point 3.2.2.1), we can deduce that the particles inserted within austenite grains of the reinforced steel are (TiMo)C carbides.  
We can thus assure that these carbides are just the same grey particles present in the carbide of the masteralloy Fe(TiMo)C added to the steel. The small difference in composition is not representative because the EDS semiquantitative analysis is not exact. Likewise, the small change in shape (less rounded in the steel) is due to erosive action of the molten steel.  
The mechanism of formation of the composite steel+carbides is the next: When the masteralloy Fe(TiMo)C contacts the liquid steel (iron base), the binder Fe of the former melts



and adds up to the metallic alloy, while the (TiMo)C particles, separated already from the binder and wetted by the liquid, remain embedded within it. Due to its high refractoriness and thermal stability, the carbide particles are not changed much even after the heat treatment of the solid material.

The polygonal titanium-molybdenum carbides, inserted metallurgically within the very ductile and tough austenite grains, decrease some mechanical characteristics (elongation, reduction of area, etc.). However, the impact energy values of the new material are sufficiently high for the expected service conditions of the typical components made in Hadfield steel (railway crossings, crushing jaws, hammers), so that, there is no risk of component fracture if this reinforced steel is used.

Besides, the beneficial effect of the carbides on the properties of the reinforced austenite such as deformability (expected to be lower, due to lower elongation), stiffness (expected to be higher, due the same reason as before), fatigue resistance (expected to be higher, due to higher yield strength), and wear resistance (clearly higher) are very interesting and promising in order to solve the characteristic shortcomings of the austenitic Hadfield steel.

In summary, the main conclusions of the present experimental work are:

- a. The powder metallurgy process SHS allows the manufacture of a masteralloy Fe(TiMo)C, wettable by molten steel and composed by particles of complex carbide in an iron binder.
- b. The addition of this masteralloy to a molten Hadfield steel bath and the subsequent solidification and heat treatment of the mix, allows the insertion of the complex carbide particles (TiMo)C of the masteralloy within the austenite grains of the steel.
- c. This insertion produces a reinforcement of the austenitic matrix, with an appreciable increase in yield strength and wear resistance, but keeps the values of the other properties, such as elongation and impact energy, within adequate levels.

In this manner, we can contribute to improve the behaviour of a material (figure 1), optimizing its properties by means of a modification of its microstructure through the combination of two metallurgical techniques of fabrication, the powder metallurgy (SHS) and the liquid metallurgy, for casting production.

## 5. Acknowledgment

This work is the result of more of 10 years of research and experimentation of a team established with the arriving of the doctor Sergei Vadchenko, an authority in the SHS field, to Inasmet (now Tecnalia). Any years later, arrived the doctor Ara Sargysan (also an specialist in powder metallurgy) substituting to the former and the development of the works increased, achieving very promising results as demonstrate the present chapter. So that, the author gratefully acknowledge these researchers, the rest people of the team and, also, the companies have financially supported several projects in this field (Fundiciones del Estanda, Talleres ZB, JEZ Sistemas Ferroviarios).

## 6. References

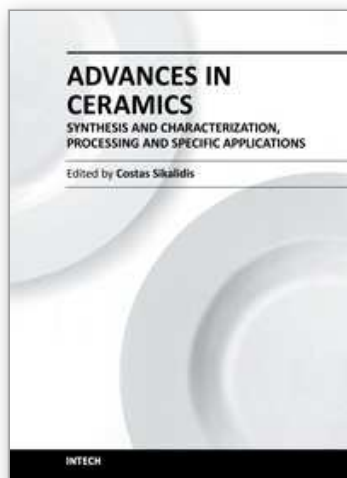
- Agote, I.; Gutierrez, M.; Orbegozo, M.; Asensio, M.; Rrausquin, J.I.; Erausquin, L.A. & Roncal, J. (2005). Desarrollo de Aceros Reforzados con Carburos Primarios Vía

- Metalurgia Liquida *Revista de Metalurgia*, Madrid, (volumen extraordinario 2005), 53-57. ISSN 0034-8570.
- Bates, P.; Walsh, M.A. & Price, S. (1998). Properties of 12% CrMoV high temperature turbine steel containing FeWTiC, *Proc. Advanced Heat Resistant Steels for Power Generation*, San Sebastián, Spain, April, 27-29, 1998.
- Chesney, P. (1990). *Metals and Materials*, New York, 373.
- Das, K.; Bandyopadhyay, T.K. & Chatterjee S. (2005). Synthesis and characterization of austenitic steel matrix composite reinforced with in-situ TiC particles. *Journal of Materials Science*, Volume 40, Number 18, (September 2005), 5007-5010.
- Degnan, C.C. & Shiway P.H. (2002). Influence of reinforcement volume fraction on sliding wear behaviour of SHS derived ferrous based metal matrix composites. *Materials Science and Technology*, Vol.18, Number 10, (October 2002), 1156-1162.
- Dogan, O.N.; Hawk, J.A.; Schrems, K.K. (2006). TiC-reinforced cast Cr steels. *Journal of materials engineering and performance*, vol. 15, n° 3, (May 2006), 320-327.
- Erausquin, J. I.; Sargysan, A. & Arana, J. L. (2009). Reinforcement of Austenitic Manganese Steel with (TiMo) Carbide Particles Previously Synthesized by SHS. *ISIJ International*, Vol. 49, No. 4 (April 2009), 582- 586.
- Erausquin, J. I (2009). Aceros Reforzados con Partículas de Carburos Primarios (TiMo)C elaboradas por SHS. Obtención Mediante Metalurgia Líquida, Conformado por Moldeo y Caracterización. *Doctoral Thesis*, Escuela Ingenieros, Bilbao, (November 2009), 56.
- Galgali R.K.; Ray H.S. & Chakrabarti A.K. (1999). Preparation of TiC reinforced steel composites and their characterization. *Materials Science and Technology*, Volume 15, Number 4, (April 1999), 437-442.
- Hathaway, R.M.; Rohatgi, P.K.; Sobczak, N. Sobczak, J. (1997). Ferrous composites: A review, *Proc. Int. Conf. High Temperature Capillarity*, Cracow, Poland, June 29-July 2, 1997.
- Kelly, A. & Macmillan, N.H. (1987). *Strong Solids*, Clarendon Pr, Oxford, 332.
- Nutting, J. (1998). The structural stability of low alloy steels for power generation applications. *Proc. Advanced Heat Resistant Steels for Power Generation*, San Sebastián, Spain, April 1998.
- Shatynski, S. R. (1979). The Thermochemistry of Transition Metal Carbides", *Oxidation of Metals*, Vol. 13, No. 2, (Mars 1979), 106.
- Steen, W.M. (1992). Future Developments of Metals and Ceramics, Institute of Materials, London, (1992), 261.
- Storms, E.K. (1967). The refractory carbides. *Academic Press*, NewYork, 1967.
- Tamburini, U.A.; Maglia, F.; Spinolo, G. Munir, Z.A. (2000). *Chimica & Industria*, (December 2000), 1.
- Terry, B.S. & Chinyamakobvu, O.S. (1992). Dispersion and reaction of TiC in liquid iron alloys. *Materials Science and Technology*, Vol. 8, (1992), 399-405.
- Tinklepaugh, J.R. & Crandall, W.B. (1960). Cermets. *Reinhfold Publishing Corporation*, New York, (1960), 146.
- Toth, L.E. (1971). Transition metal carbides and nitrides. *Academic Press*, NewYork, 1971.

Wood, J.V.; Dinsdale, K.; Davies, P. & Kellie, J.L.F. (1995). Production and properties of steel-TiC composites for wear applications. *Materials Science and Technology*, Vol. 11, (1995), 1315-1320.

IntechOpen

IntechOpen



**Advances in Ceramics - Synthesis and Characterization,  
Processing and Specific Applications**

Edited by Prof. Costas Sikalidis

ISBN 978-953-307-505-1

Hard cover, 520 pages

**Publisher** InTech

**Published online** 09, August, 2011

**Published in print edition** August, 2011

The current book contains twenty-two chapters and is divided into three sections. Section I consists of nine chapters which discuss synthesis through innovative as well as modified conventional techniques of certain advanced ceramics (e.g. target materials, high strength porous ceramics, optical and thermo-luminescent ceramics, ceramic powders and fibers) and their characterization using a combination of well known and advanced techniques. Section II is also composed of nine chapters, which are dealing with the aqueous processing of nitride ceramics, the shape and size optimization of ceramic components through design methodologies and manufacturing technologies, the sinterability and properties of ZnNb oxide ceramics, the grinding optimization, the redox behaviour of ceria based and related materials, the alloy reinforcement by ceramic particles addition, the sintering study through dihedral surface angle using AFM and the surface modification and properties induced by a laser beam in pressings of ceramic powders. Section III includes four chapters which are dealing with the deposition of ceramic powders for oxide fuel cells preparation, the perovskite type ceramics for solid fuel cells, the ceramics for laser applications and fabrication and the characterization and modeling of protonic ceramics.

**How to reference**

In order to correctly reference this scholarly work, feel free to copy and paste the following:

Jose Ignacio Erasquin (2011). Reinforcement of Austenitic Manganese Steel with (TiMo) Carbide Particles Previously Synthesized by SHS, *Advances in Ceramics - Synthesis and Characterization, Processing and Specific Applications*, Prof. Costas Sikalidis (Ed.), ISBN: 978-953-307-505-1, InTech, Available from: <http://www.intechopen.com/books/advances-in-ceramics-synthesis-and-characterization-processing-and-specific-applications/reinforcement-of-austenitic-manganese-steel-with-timo-carbide-particles-previously-synthesized-by-sh>

**INTeCH**  
open science | open minds

**InTech Europe**

University Campus STeP Ri  
Slavka Krautzeka 83/A  
51000 Rijeka, Croatia  
Phone: +385 (51) 770 447  
Fax: +385 (51) 686 166

**InTech China**

Unit 405, Office Block, Hotel Equatorial Shanghai  
No.65, Yan An Road (West), Shanghai, 200040, China  
中国上海市延安西路65号上海国际贵都大饭店办公楼405单元  
Phone: +86-21-62489820  
Fax: +86-21-62489821

[www.intechopen.com](http://www.intechopen.com)

IntechOpen

IntechOpen



© 2011 The Author(s). Licensee IntechOpen. This chapter is distributed under the terms of the [Creative Commons Attribution-NonCommercial-ShareAlike-3.0 License](https://creativecommons.org/licenses/by-nc-sa/3.0/), which permits use, distribution and reproduction for non-commercial purposes, provided the original is properly cited and derivative works building on this content are distributed under the same license.

IntechOpen

IntechOpen